

Article

Not peer-reviewed version

Intraspecific Drought Stress Responses Detected Using Remotely Sensed Vegetation Indices in Sitka Spruce (*Picea sitchensis*)

[Gerrard English](#)*, [Jacqueline Rosette](#), [Juan Suárez](#)

Posted Date: 10 April 2026

doi: 10.20944/preprints202604.0570.v1

Keywords: remote sensing; drought; hyperspectral; sitka spruce; forestry



Preprints.org is a free multidisciplinary platform providing preprint service that is dedicated to making early versions of research outputs permanently available and citable. Preprints posted at Preprints.org appear in Web of Science, Crossref, Google Scholar, Scilit, Europe PMC.

Copyright: This open access article is published under a [Creative Commons CC BY 4.0 license](#), which permit the free download, distribution, and reuse, provided that the author and preprint are cited in any reuse.

Disclaimer/Publisher's Note: The statements, opinions, and data contained in all publications are solely those of the individual author(s) and contributor(s) and not of MDPI and/or the editor(s). MDPI and/or the editor(s) disclaim responsibility for any injury to people or property resulting from any ideas, methods, instructions, or products referred to in the content.

Article

Intraspecific Drought Stress Responses Detected Using Remotely Sensed Vegetation Indices in Sitka Spruce (*Picea sitchensis*)

Gerrard English ^{1,*}, Jacqueline Rosette ¹ and Juan Suárez ²

¹ Swansea University, Swansea, UK, SA2 8PP

² Forest Research, Northern Research Station, Roslin, UK, EH25 9SY

* Correspondence: g.j.english@swansea.ac.uk or gerrardenglish93@gmail.com

Highlights

What are the main findings?

- Hyperspectral vegetation indices detected clear intraspecific variation in drought response, revealing distinct clonal strategies (avoidance vs tolerance) in Sitka spruce.
- Pigment and red-edge indices were sensitive to drought, providing early and sustained signals of stress, while NDVI showed little response.

What are the implications of the main findings?

- Proximal hyperspectral sensing enables rapid, non-destructive screening of drought resilience, supporting integration into forest breeding programmes for climate adaptation.
- Drought monitoring approaches should prioritise pigment and red-edge indices over NDVI, improving early detection of physiological stress in forest systems.

Abstract

UK forestry faces increasing drought risk under climate change, raising concerns about the resilience of Sitka spruce, the UK's dominant commercial conifer. This study assessed whether hyperspectral vegetation indices can detect intraspecific drought responses to support resilience screening. An eight-week controlled drought experiment was conducted on six clonal groups, using needle-level hyperspectral reflectance to derive indices of chlorophyll status, photoprotective pigments, and water content, alongside chlorophyll fluorescence (Fv/Fm). Drought responses were detected across multiple indices, with pigment-based and red-edge indices showing the earliest and strongest sensitivity, while water-related indices captured later-stage hydraulic decline. Significant clonal variation was observed in the timing and magnitude of pigment regulation, water loss, and photosynthetic impairment, indicating contrasting drought response strategies. These results demonstrate that hyperspectral approaches enable rapid, non-destructive detection of physiologically meaningful drought responses and can support the identification of drought-resilient genotypes for climate-adaptive forest management.

Keywords: remote sensing; drought; hyperspectral; sitka spruce; forestry

1. Introduction

Climate change is increasing drought frequency across Europe, reducing forest productivity [1]. Increasingly dry summers pose challenges to UK commercial forestry [2,3]. The long-lived nature of trees makes forests vulnerable to extreme weather events, creating high maladaptation costs [4]. Selecting drought-resilient planting material is therefore central to climate-adaptive forest management.

Sitka spruce (*Picea sitchensis* (Bong.) Carr) is the dominant plantation species in the UK and, together with Ireland, covers over one million hectares [5]. It is widely used for replanting and afforestation but, relative to other commercial conifers, can be susceptible to drought [4,6].

Recent drought events have impacted Sitka spruce. During the extreme European drought of 2003, widespread damage and mortality were recorded across north-eastern Scotland [7,8]. In the warm, dry spring and summer of 2018, photosynthesis in a mature plantation decreased by 5%, and mortality of seedlings increased following reforestation [1]. Summers similar to 2018 are projected to become typical in the UK by 2050 [9], raising concerns about the long-term climatic suitability of Sitka spruce across parts of the UK.

Intraspecific drought response is critical for understanding species resilience under climate change. The Sitka spruce breeding programme, established in 1963, has successfully improved timber quality [10]. Due to its high productivity, Sitka spruce is still likely to be favoured across much of the UK in the near future [11]. Integrating drought tolerance screening into breeding programmes may provide a scalable pathway to enhance forest resilience without requiring species replacement [12].

Remotely sensed hyperspectral approaches have been widely used to detect drought stress; however, their application to characterising intraspecific drought variation in commercially important forestry species remains limited. In particular, the potential to detect clonal differences in drought response using reflectance-based metrics has received relatively little attention in commercial forestry contexts.

This study investigates the application of hyperspectral vegetation indices (VI) to quantify clone-level variation in drought responses within Sitka spruce under controlled progressive drought. Specifically, we aim to (i) identify VI responsive to progressive drought stress, (ii) determine whether clonal differences in drought response can be detected spectrally, and (iii) evaluate whether pigment and water-related indices capture contrasting drought response strategies among clones. These findings have implications for the development of rapid, non-destructive drought resilience screening tools within forest breeding programmes.

2. Materials and Methods

2.1. Study Location and Plant Material

The experiment was conducted in a polytunnel located at the Forest Research Northern Research Station, Scotland, UK, during the summer of 2022, allowing for control of plant water inputs. A temperature-operated fan increased air flow and cooled the environment.

Sitka spruce plants were taken from the Forest Research clonal archive (Roslin, UK). Sixty trees were used, consisting of ten ramets from six clonal groups. Ramets originated from scions, collected from mature grafts of original breeding population trees from west Scotland and southwest England. Two clonal groups are part of the general breeding population in the UK. Scions were grafted to rootstock in 2015 and planted in 9.5 L pots in 'nursery stock general' soil (ICL, Suffolk) with slow-release fertiliser (120 N, 60 P, and 199 K mg L⁻¹). Scions were randomly assigned to control or drought treatments and moved to the polytunnel in late May 2022.

2.2. Spectra Collection

Needle reflectance spectra were collected weekly for the duration of the experiment (7th June - 24th August 2022), using a field spectroradiometer (ASD FieldSpec 4 standard Res, Analytik Ltd, Cambridge) sampling wavelengths in the range of 350 - 2500 nm (3 -10 nm resolution). Non-destructive sampling was required to maintain full canopies and avoid stress associated with high levels of defoliation.

Needles were arranged to form a flat, continuous surface over an ASD contact probe using low-reflectance gloves to minimise external light contamination. The probe was repositioned between measurements to reduce orientation bias [13]. Five measurements (25 rapidly collected spectra) were

averaged to generate a single representative spectrum. Due to the regular needle arrangement, predominantly upward-facing surfaces were sampled.

Overwintered needles from the previous year's growth (2021) taken in the top 25% of the vertical canopy profile were sampled. Current year needles were excluded due to high spectral variation during expansion [14]. Needle age is determined by counting internodes backwards, from the current year [15]. A white reference was taken every 15 minutes using a 99% Spectralon panel. Sampling equipment was routinely assessed and cleaned to avoid contamination.

2.3. Spectra Processing

Spectra were interpolated to 1 nm and converted to absolute reflectance (R_{abs}) by,

$$R_{abs} = \frac{R_{sample}}{DN_{WR}} \times R_{WR}, \quad (1)$$

where R_{sample} is the raw spectra, DN_{WR} is the white reference taken in the field and R_{WR} is a lab calibrated reflectance value (NERC field spectroscopy facility, Edinburgh, UK).

Vegetation indices (VI) provide physiologically interpretable metrics and reduce spectral dimensionality. They were taken from the literature and are categorised as: Greenness VI (VIg) sensitive to chlorophyll concentration, Pigment VI (VIp) sensitive to stress-related pigments (carotenoids and anthocyanins), and Water Content VI (VIw) which are sensitive to water content. See Table S1 for the selected VI and their formulae.

2.4. Soil Moisture and Watering Regime

Soil moisture was monitored using ThetaProbe ML2x sensors (Delta-T Devices Ltd, Cambridge, UK). Continuous measurements were recorded every 30 minutes using a CR1000x datalogger (Campbell Scientific, Shepshed, UK). One tree per clonal group per treatment was equipped with an *in-situ* probe. Manual measurements were also taken two to three times per week using an ML2x sensor connected to an HH2 meter. Three readings per pot were averaged to estimate soil moisture. A soil-specific calibration was applied following manufacturer guidance.

Prior to treatment initiation, field capacity (FC) was determined for each pot by saturating soil and allowing drainage for two hours. Control plants were maintained at 80–100% FC. Drought treatments were imposed gradually. During weeks 1–2, soil moisture declined to approximately 20–25% FC and was maintained at that level. Thereafter, pots were watered to 20% FC once weekly before being left unwatered for the remainder of the drought period.

2.5. Chlorophyll Fluorescence (F_v/F_m)

Maximal photochemical efficiency of photosystem II (F_v/F_m) was measured with a Pulse-Amplitude-Modulation (PAM) chlorophyll fluorometer (MINI-PAM-II, H. Walz, Effeltrich, Germany). F_v/F_m was calculated as,

$$F_v/F_m = \frac{F_m - F_o}{F_m}, \quad (2)$$

where F_o is the minimum fluorescence and F_m is the maximum fluorescence in the dark-adapted state. Needles were dark acclimated for 30 minutes using a leaf clip (DLC-8). F_o is taken using a low intensity measuring light. F_m is taken immediately after a 0.8 s saturating pulse.

2.6. Statistical Analysis

To assess the effects of drought and clonal group on VI, a Bayesian quadratic regression model was fitted for each VI using a Gaussian likelihood implemented in the R package brms. Fixed effects included treatment (control or drought), clonal group, and time since drought initiation (in days), together with their interactions. A second order polynomial term for time was included to capture non-linear temporal responses. Time was standardised (mean = 0, SD =1) prior to model fitting, and

the clonal group was fitted using zero-to-sum contrasts. Random intercepts and time slopes were included for individual trees to account for repeated measures.

For each VI, the intercept was assigned a weakly informative normal prior centred on expected magnitude of that index, reflecting known index ranges and ensuring realistic baseline estimates. All fixed-effect coefficients were assigned zero-centred weakly informative normal priors. Random-effect standard deviations were assigned weakly informative priors on the positive scale. Prior scales were adjusted across indices to account for differences in response magnitude.

Four Markov chain Monte Carlo chains run for 1,000 warm-up and 3,000 post-warm-up samples per chain. Checks of chain convergence and posterior predictive ability were performed on all models.

Fv/Fm was analysed using linear mixed-effects models to account for repeated measurements on individual trees. Time since drought initiation was treated as a continuous variable and modelled using natural splines ($df = 3$), with spline complexity selected based on Akaike's Information Criterion (AIC), to accommodate non-linear temporal responses. Fixed effects included time, treatment, clone, and their interactions, and tree identity was included as a random intercept to account for within-tree dependence.

3. Results

3.1. Temporal Trends

Over the experimental period most VI exhibited clear linear temporal trends independent of watering treatment (Figure 1, S1, S2, S2). Evidence for non-linear temporal effects was strongest for ARI1, while ARI2 showed weaker support. No evidence for change over time was found for CIgr and WI. No consistent evidence of clone-specific temporal responses independent of treatment was observed (Figure S1, S2, S3).

3.2. Vegetation Indices

No consistent drought response was detected in NDVI, with posterior estimates centred near zero (Figure 1, S1). In contrast, red-edge indices exhibited consistent declines under drought. Maximum treatment differences reached 0.22 (95% CI: 0.03-0.41) for CIre and 0.05 (95% CI: 0.02-0.08) for NDVIre by day 57. Declines accelerated over time, resulting in progressive separation between droughted and control plants (Figure 1).

All stress-pigment vegetation indices (VIp) exhibited strong drought responses, with posterior treatment contrasts clearly separated from zero (Figure 1, S2). Divergence between treatments was evident early and increased over time. By the midpoint of the experiment, ARI1 and ARI2 had diverged by 0.48 (95% CI: 0.34-0.62) and 0.33 (95% CI: 0.25-0.42), respectively, under drought relative to controls, while PRI differed by 0.015 (95% CI: 0.01-0.02). PRI and CCI displayed predominantly linear temporal responses, whereas ARI1 and ARI2 showed evidence of non-linear (decelerating) dynamics (Figures 1, S2, S5).

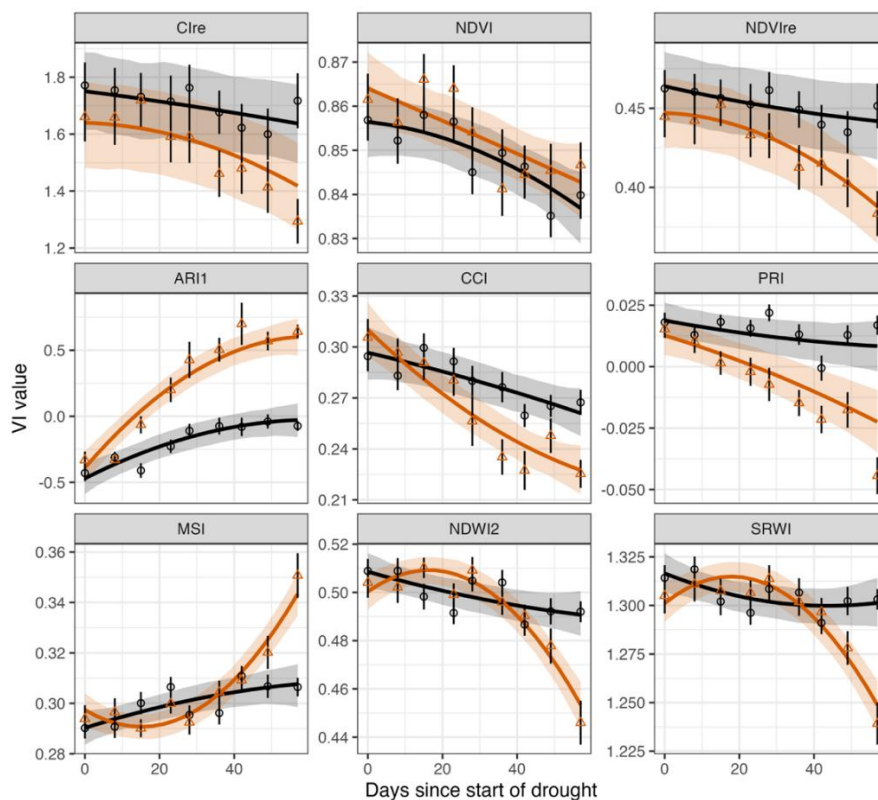


Figure 1. Selected Sitka spruce Vegetation Indices (VI) responses over time. Points are average VI values (\pm SE). Solid lines and shaded bands represent modelled posterior means and 95% credible intervals. Black points and lines represent the control group while orange points and lines are the drought group. Divergence between treatments over time indicates progressive drought effects. Full model outputs for all vegetation indices are provided in the Supplementary Material.

All water-related vegetation indices (VI_w) diverged between droughted and control plants (Figures 1, S3). Treatment responses were generally quadratic, characterised by initial increases during the first half of the experiment followed by marked declines as drought progressed (Figures 1, S6). MSI exhibited the inverse pattern due to its formulation.

NDWI2 and SRWI showed the strongest drought responses, decreasing relative to controls, whereas MSI increased under drought. In contrast, NDWI1, WI, and WI/NDVI displayed weaker overall treatment effects, with credible intervals for linear treatment terms overlapping zero (Figure S3).

3.3. Clone Effects

Clear intraspecific variation in drought response was detected across pigment and water-related vegetation indices. Clone 6 exhibited a stronger pigment-based drought response than the clonal mean, with pronounced increases in ARI1 and ARI2 during the early stages of drought, PRI responses in Clone 6 also diverged from the average clonal pattern, showing a sharper decline under drought (Figure 2). By the midpoint of the experiment, ARI1 and ARI2 had diverged by 1.2 (95% CI: 0.86-1.52) and 0.83 (95% CI: 0.61-1.05), respectively, under drought relative to controls, while PRI differed by 0.05 (95% CI: 0.03-0.07).

Water-related indices revealed contrasting clonal responses. Clone 2 showed the strongest divergence from the mean drought response across MSI, NDWI1, NDWI2, SRWI, and WI, characterised by greater linear deviation from control and altered response shape (Figure 2, S9). Clone

1 also deviated from the mean response across several VIw, although these differences were smaller in magnitude and less consistent than those observed for Clone 2 (Figure 2).

Additional clone-specific differences in response shape were observed for Clones 3 and 4. Clone 3 displayed non-linear deviations from the mean drought response across several VIw, whereas Clone 4 showed limited divergence, with shape differences evident in SRWI (Figure 2).

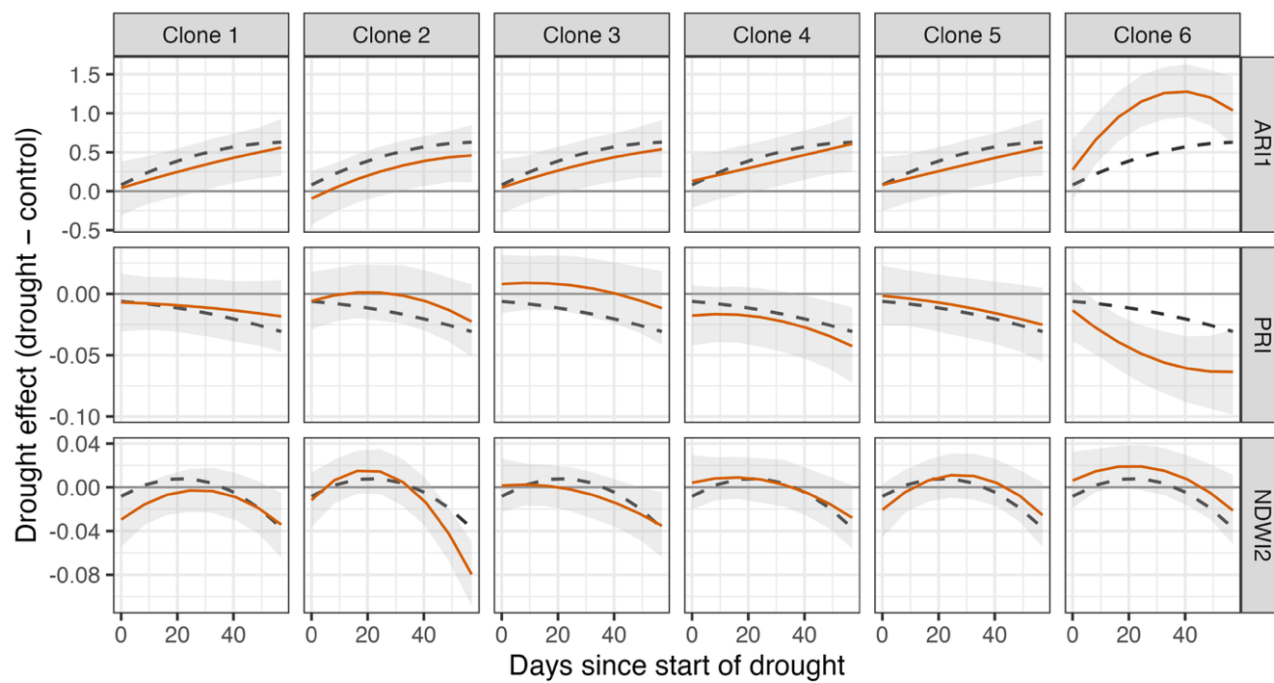


Figure 2. Modelled clonal drought response for selected Vegetation Indices (VI). Drought effect is the modelled difference between the control and drought group. Coloured lines and shaded bands represent posterior means and 95% credible intervals for each clone. Dashed lines represent the mean clonal response. The horizontal line indicates zero effect. Full model outputs for all vegetation indices are provided in the Supplementary Material.

3.4. Chlorophyll Fluorescence (F_v/F_m)

F_v/F_m exhibited non-linear temporal dynamics over the course of the experiment. Under control conditions, F_v/F_m remained relatively stable across clones, whereas droughted plants showed progressive reductions in photosynthetic efficiency (Figure 3). A significant time \times treatment \times clone interaction indicated that drought-induced trajectories differed among clones.

Divergence between control and drought treatments occurred earliest in Clone 6 (approximately day 23), followed by Clone 4 (around day 30). In contrast, Clones 2 and 3 did not exhibit significant treatment separation until later in the experiment (day 49), while Clones 1 and 5 showed significant reductions only at the final sampling date (day 56). The magnitude of late-stage decline was greatest in Clones 2 and 4, consistent with pronounced reductions in photosystem II efficiency under sustained drought. Clone 1 displayed the smallest overall change in F_v/F_m throughout the experimental period.

In several clones, transient mid-experiment reductions in F_v/F_m were followed by partial recovery prior to further decline, indicating short-term physiological adjustments potentially exacerbated by fluctuations in polytunnel conditions.

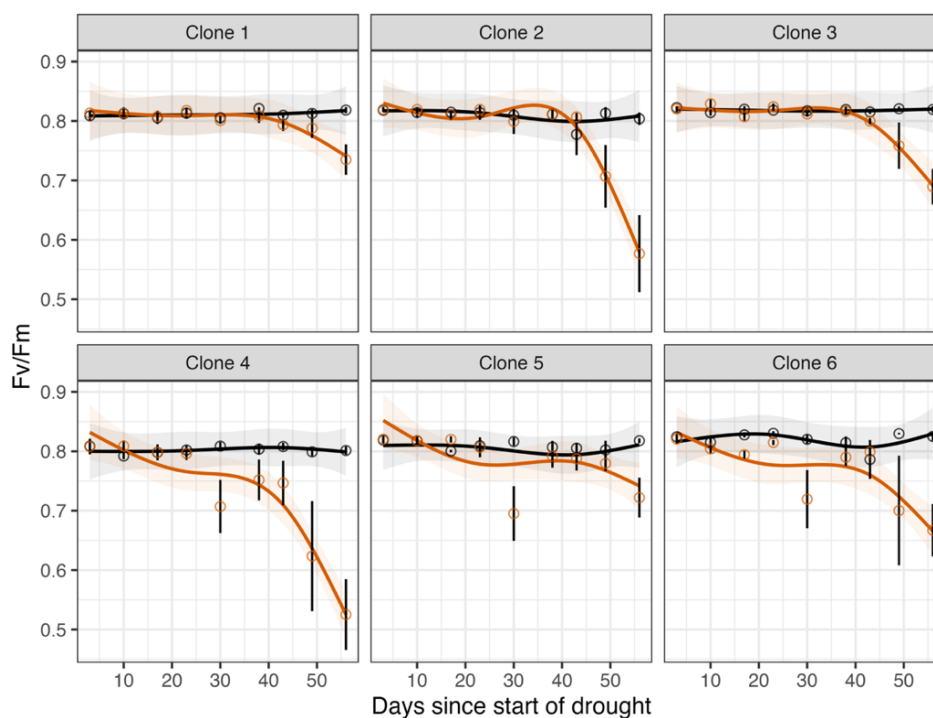


Figure 3. Clonal maximum photochemical efficiency (F_v/F_m) response over time. Points are average measurements (\pm SE). Lines and shading are the modelled response and 95% confidence interval. Orange lines and points are the drought group while black points and lines are the control.

4. Discussion

4.1. Chlorophyll and Greenness Response

The combination of hyperspectral Vegetation Indices (VI) provides a biophysical picture of drought response in Sitka spruce. Drought responses were detected in all VI except NDVI. Chlorophyll-associated (VIg) decreased or remained stable under drought, pigment indices (Vip) indicated higher photoprotective pigment expression, and water content indices (VIw) captured foliar water loss in the latter half of the drought.

NDVI, the most widely used VI, was insensitive to drought stress in the present study. NDVI is sensitive to green leaf area and canopy structure but can saturate in evergreen canopies [16]. Although some defoliation was observed in this study - an emergency response in conifers - the needle-level measurements do not capture canopy parameters such as leaf area index (LAI) [17]. This likely explains the lack of response in NDVI observed here.

In contrast, red-edge indices (CIre and NDVIre) declined steadily under drought. The red-edge region (approximately 680–750 nm) represents a transition zone between strong chlorophyll absorption and high near-infrared reflectance. As chlorophyll concentration decreases, the red-edge shifts toward shorter wavelengths, reducing saturation effects and increasing sensitivity to subtle pigment variation [18–20]. The stronger response of CIre and NDVIre therefore likely reflects enhanced sensitivity to needle-level chlorophyll decline.

The drought response of CIgr (which uses green light reflectance) was weaker than the red-edge indices. Green light penetrates more deeply into leaf tissue and is absorbed less efficiently than red wavelengths [21]. Chloroplasts in the upper cell layers experience the greatest excess light and photoinhibition. Chloroplasts contributing to green reflectance may therefore experience reduced excess energy relative to those in upper cell layers, potentially limiting the magnitude of drought-induced change detected by CIgr [22].

4.2. Photoprotective Pigment Dynamics

PRI and CCI declined under drought stress and are closely associated with carotenoid dynamics, specifically the xanthophyll cycle. Xanthophyll pigments change the distribution of absorbed light at 531 nm in response to changes in energy dissipation [16,23]. During stress, excess absorbed energy is dissipated as heat via the de-epoxidation of violaxanthin to zeaxanthin, while the reverse reaction occurs under non-saturating light conditions [24,25]. The observed decline in PRI and CCI is therefore consistent with enhanced non-photochemical quenching under drought, a response widely reported across conifer species [26–30].

The drought response of the two anthocyanin-based VI was among clearest of all the selected VI. Separation between the control and drought group was evident after two weeks and increased for the remainder of the experiment. Increased ARI1 and ARI2 indicate elevated anthocyanin concentrations, reflecting enhanced photoprotection as plants acclimate to stressful conditions. The anthocyanin drought response was rapid and sustained, suggesting that regulation of these pigments is important in Sitka spruce across mild to severe drought stress. Pigment-based responses preceded detectable declines in Fv/Fm in several clones, indicating that photoprotective adjustments were initiated before measurable impairment of photosystem II efficiency.

There are uncertainties surrounding the exact role of anthocyanins under drought stress [31–33]. However, substantial evidence supports a light screening function, whereby photoinhibition is reduced through absorption of high-energy photons and shielding light-saturated photosynthetic machinery [32,34,35]. Antioxidant roles have also been proposed, although this is under debate [31,36].

4.3. Foliar Water Dynamics

All water-related indices (VIw) exhibited a similar pattern during the drought treatment. Initially, VIw decreased relative to the control, then sharply diverged from days 30–40. These indices are correlated with foliar water content and water potential in conifers [37]. The rapid shift observed in the latter stages of the experiment suggests substantial needle water loss once plants were no longer able to maintain hydraulic function.

The initial increase in water content relative to controls was unexpected. Declines in water content in conifer needles under stress can be slow [38]. It is hypothesised that in the early stages of drought, stomatal closure reduced transpiration sufficiently to maintain relatively high needle water potential. This is analogous to elevated pre-dawn water potential when stomata close overnight [39]. Past a certain drought stress threshold [40] however, hydraulic regulation appears to fail and needle desiccation progressed rapidly.

These findings suggest that VIw are sensitive indicators of severe water limitation but may be less reliable during early or moderate stress. Further work combining spectral indices with direct measurements of needle water content and water potential would help clarify the temporal dynamics of hydraulic decline in Sitka spruce.

WI/NDVI displayed the weakest drought response of all VIw, likely reflecting the inclusion of NDVI in its formulation, which was insensitive to drought under the present experimental conditions.

4.4. Maximal Photosynthetic Capacity and Clonal Variation

Declines in Fv/Fm under drought occurred non-linearly and varied among clones, with divergence between treatments emerging at different stages of the experiment. Early separation was detected in Clones 4 and 6, whereas Clones 2 and 3 only exhibited significant divergence during the later stages of drought, and Clones 1 and 5 showed treatment differences only at the final sampling date. These contrasting temporal patterns suggest differences in the thresholds at which photosystem II efficiency becomes impaired under sustained water limitation.

In some clones, transient mid-experiment reductions in Fv/Fm were followed by partial recovery prior to further decline, indicating short-term physiological adjustment potentially influenced by fluctuations in polytunnel environmental conditions, as previously recorded in Sitka spruce [41]. Such temporary reductions are consistent with reversible photoinhibition rather than irreversible photodamage [42].

The delayed but severe collapse observed in Clones 2 and 4 may reflect hydraulic failure following prolonged drought, whereas the relative stability of Clone 1 suggests greater drought avoidance or more effective maintenance of photochemical function under stress.

4.5. Clonal Differences in Drought Strategy

Evidence of clonal variation in drought response was most apparent in pigment- and water-related vegetation indices. Clone 6 exhibited a stronger drought-induced pigment response relative to other clones and was among the first to display divergence in Fv/Fm. In contrast, Clone 2 showed a relatively modest early pigment response but experienced the most pronounced decline in VIw and a late and steep reduction under drought stress.

Via different mechanisms, Clones 2 and 6 exhibited stronger drought responses than the other clonal groups. The more extreme VIw response in Clone 2 suggests reduced capacity to avoid drought stress until favourable conditions return. Maintenance of leaf water content and hydraulic integrity through stomatal regulation represents a primary drought avoidance strategy, as photosynthesis and growth are constrained to conserve water [43]. However, a plant's capacity to avoid drought is limited by drought duration and intensity.

In contrast, pigment regulation under drought is more characteristic of tolerance strategies, whereby plants acclimate to sustained stress while attempting to maintain metabolic function [44]. Enhanced energy dissipation, osmotic adjustment and antioxidative protection all contribute to maintaining photosynthetic function under sub-optimal conditions. Clone 6 rapidly upregulated anthocyanins and exhibited strong xanthophyll cycle responses, suggesting a lower drought threshold for activating photoprotective mechanisms.

Clone 1 appeared least affected by the experimental drought. Treatment differences in Fv/Fm were only detectable by the final week and were relatively small in magnitude. Relatively modest changes in VIw were also detected in Clone 1, suggesting lesser drought susceptibility, via greater drought avoidance capacity or more stable photosynthetic efficiency under declining water availability.

Intraspecific drought responses are widespread in conifers [45–48], including Sitka spruce [49]. However, evaluation of this variation using remotely sensed spectral indices is rare [50,51]. Vegetation indices have been successfully applied to identify drought-tolerant varieties in agricultural crops [52,53] however, despite increasing use of hyperspectral methods in forest monitoring, their application to assessing intraspecific drought tolerance in conifers remains limited.

Collectively, these patterns indicate distinct drought response strategies within a selection of breeding population clones. Clone 6 exhibited early and sustained photoprotective pigment regulation consistent with a tolerance strategy, Clone 2 showed delayed but pronounced hydraulic decline indicative of avoidance failure under sustained stress, and Clone 1 maintained relatively stable physiological function throughout the experiment. These contrasting trajectories highlight substantial intraspecific variation in drought response mechanisms within Sitka spruce.

4.6. Seasonal and Temporal Trends

Temporal trends were detected across most vegetation indices irrespective of drought treatment, reflecting seasonal adjustment in needle biochemistry. Evergreen conifers regulate photosynthetic capacity primarily through pigment pool adjustments rather than canopy senescence (Gamon et al., 2016). Seasonal declines in chlorophyll and concurrent increases in carotenoid and xanthophyll pools can elevate visible reflectance as summer progresses [16,54], consistent with patterns observed in both treatments during the present study.

Subtle seasonal changes in needle water content may also influence SWIR reflectance [55]. A slight increase over the season in the SWIR recorded by Qi et al. (2014) is comparable to the spectra collected here. These temporal trends were evident in both control and drought treatments, demonstrating that seasonal adjustment was distinct from drought specific responses.

4.7. Implications for Breeding and Management

The present analysis demonstrates that hyperspectral vegetation indices can detect physiologically meaningful drought responses in Sitka spruce and differentiate clonal strategies under sustained water limitation. This could facilitate non-destructive screening of drought resilience, supporting integration into forest breeding programmes for climate adaptation. Pigment-related indices were particularly sensitive to progressive stress, while water-related indices captured late-stage hydraulic decline. These spectral responses aligned with divergence in Fv/Fm, indicating that reflectance-based metrics tracked underlying changes in photochemical efficiency.

Among VI_p, PRI tracked xanthophyll cycle dynamics consistently, reinforcing its value as a marker of photoprotection under stress [27–30]. Anthocyanin-based indices detected early stress responses and show clear separation between control and drought treatments. Because anthocyanins are less directly linked to photosynthetic efficiency than carotenoids, they may provide a more stress-specific signal in evergreen conifers, where seasonal canopy senescence does not confound reflectance patterns.

5. Conclusions

The hyperspectral VI identified clear pigment and water-related drought responses in Sitka spruce that varied at the clonal level. Variation in photoprotective pigment dynamics revealed contrasting drought response mechanisms among clones, with rapid anthocyanin upregulation emerging as a sensitive early biomarker of stress alongside detection of xanthophyll cycle activity through PRI. Water-related indices indicated a more complex trajectory, with apparent maintenance or transient accumulation of needle water during early drought, consistent with avoidance strategies, followed by rapid desiccation as stress intensified. Clones differed not only in the magnitude of drought susceptibility but also in the mechanisms deployed, with some exhibiting pronounced pigment-based photoprotective adjustment and others showing stronger hydraulic decline.

The integration of pigment, water, and chlorophyll fluorescence signals revealed distinct drought response strategies within the breeding population, ranging from early photoprotective regulation to delayed but severe physiological collapse. Such differentiation is directly relevant to breeding programmes aiming to identify genotypes with enhanced drought avoidance or tolerance. The capacity to screen large populations using rapid, non-destructive hyperspectral methods provides a scalable approach for high-throughput phenotyping and supports the development of more drought-resilient planting material for climate-adaptive forest management.

Supplementary Materials: The following supporting information can be downloaded at the website of this paper posted on Preprints.org, Figure S1: Key determinants of Sitka spruce greenness vegetation index variation; Figure S2: Key determinants of Sitka spruce pigment vegetation index variation; Figure S3: Key determinants of Sitka spruce water content vegetation index variation; Figure S4 Sitka spruce greenness vegetation index responses over time; Figure S5 Sitka spruce pigment vegetation index responses over time; Figure S4 Sitka spruce water content vegetation index responses over time; Figure S7 Modelled clonal drought responses for greenness vegetation indices; Figure S8 Modelled clonal drought responses for pigment vegetation indices; Figure S9 Modelled clonal drought responses for water content vegetation indices.

Author Contributions: Conceptualisation, Data curation and Validation, Formal analysis Investigation, Methodology, Visualisation, Writing – original draft: G.E.; Supervision, Project administration, Writing – review & editing: J.R.; Conceptualisation, Supervision, Resources, Writing – review & editing: J.S. All authors have read and agreed to the published version of the manuscript.

Funding: This research received no external funding.

Data Availability Statement: Dataset available on request from the authors.

Acknowledgments: The authors have reviewed and edited the output and take full responsibility for the content of this publication.”

Conflicts of Interest: The authors declare no conflicts of interest.

Abbreviations

Fv/Fm	Maximal photochemical efficiency of photosystem II
VI	Vegetation Index
VIg	Greenness vegetation index
VIp	Pigment vegetation index
VIw	Water content vegetation index
FC	Field capacity
AIC	Akaike’s Information Criterion

References

- Xenakis, G.; Ash, A.; Siebicke, L.; Perks, M.; Morison, J.I.L. Comparison of the Carbon, Water, and Energy Balances of Mature Stand and Clear-Fell Stages in a British Sitka Spruce Forest and the Impact of the 2018 Drought. *Agric. For. Meteorol.* **2021**, *306*, 108437, doi:10.1016/j.agrformet.2021.108437.
- Burke, E.J.; Perry, R.H.J.; Brown, S.J. An Extreme Value Analysis of UK Drought and Projections of Change in the Future. *J. Hydrol.* **2010**, *388*, 131–143, doi:10.1016/j.jhydrol.2010.04.035.
- Met Office UK Climate Projections: Headline Findings. **2021**, 1–12.
- Locatelli, T.; Beauchamp, K.; Perks, M.; Xenakis, G.; Nicoll, B.; Morison, J. Drought Risk in Scottish Forests 2021.
- Mason, W. Implementing Continuous Cover Forestry in Planted Forests: Experience with Sitka Spruce (*Picea Sitchensis*) in the British Isles. *Forests* **2015**, *6*, 879–902, doi:10.3390/f6040879.
- Samuel, S.; Fletcher, A.M.; Lines, R. *Choice of Sitka Spruce Seed Origins for Use in British Forests*; Bulletin / Forestry Commission; Forestry Commission: Edinburgh, 2007; ISBN 978-0-85538-727-3.
- Green, S.; Hendry, S.; Redfern, D. Drought Damage to Pole-Stage Sitka in NE Scotland. *Scott. For.* **2008**, *62*, 10–18.
- Green, S.; Ray, D. Potential Impacts of Drought and Disease on Forestry in Scotland. *For. Res.* **2009**, 1–8.
- Betts, R.A.; Brown, K. The Third UK Climate Change Risk Assessment (CCRA3) Technical Report. *UK Clim. Risk* **2021**.
- Lee, S. Improving the Timber Quality of Sitka Spruce through Selection and Breeding. *Forestry* **1999**, *72*, 123–146, doi:10.1093/forestry/72.2.123.
- Davies, S.; Bathgate, S.; Petr, M.; Gale, A.; Patenaude, G.; Perks, M. Drought Risk to Timber Production – A Risk versus Return Comparison of Commercial Conifer Species in Scotland. *For. Policy Econ.* **2020**, *117*, 102189, doi:10.1016/j.forpol.2020.102189.
- Schiop, S.T.; Al Hassan, M.; Sestras, A.F.; Boscaiu, M.; Sestras, R.E.; Vicente, O. Biochemical Responses to Drought, at the Seedling Stage, of Several Romanian Carpathian Populations of Norway Spruce (*Picea Abies* L. Karst). *Trees - Struct. Funct.* **2017**, *31*, 1479–1490, doi:10.1007/s00468-017-1563-1.
- Serbin, S.P.; Singh, A.; McNeil, B.E.; Kingdon, C.C.; Townsend, P.A. Spectroscopic Determination of Leaf Morphological and Biochemical Traits for Northern Temperate and Boreal Tree Species. *Ecol. Appl.* **2014**, *24*, 1651–1669, doi:10.1890/13-2110.1.
- Wu, Qiaoli.; Song, C.; Song, Jinling.; Wang, Jindi.; Chen, Shaoyuan.; Yu, Bo. Impacts of Leaf Age on Canopy Spectral Signature Variation in Evergreen Chinese Fir Forests. *Remote Sens.* **2018**, *10*, 262, doi:10.3390/rs10020262.
- O’Neill, A.L.; Kupiec, J.A.; Curran, P.J. Biochemical and Reflectance Variation throughout a Sitka Spruce Canopy. *Remote Sens. Environ.* **2002**, *80*, 134–142, doi:10.1016/S0034-4257(01)00294-2.

16. Gamon, J.A.; Huemmrich, K.F.; Wong, C.Y.S.; Ensminger, I.; Garrity, S.; Hollinger, D.Y.; Noormets, A.; Peñuelask, J. A Remotely Sensed Pigment Index Reveals Photosynthetic Phenology in Evergreen Conifers. *Proc. Natl. Acad. Sci. U. S. A.* **2016**, *113*, 13087–13092, doi:10.1073/pnas.1606162113.
17. Nadal-Sala, D.; Grote, R.; Birami, B.; Knüver, T.; Rehschuh, R.; Schwarz, S.; Ruehr, N.K. Leaf Shedding and Non-Stomatal Limitations of Photosynthesis Mitigate Hydraulic Conductance Losses in Scots Pine Saplings During Severe Drought Stress. *Front. Plant Sci.* **2021**, *12*, 715127, doi:10.3389/fpls.2021.715127.
18. Clevers, J.G.P.W.; Gitelson, A.A. Remote Estimation of Crop and Grass Chlorophyll and Nitrogen Content Using Red-Edge Bands on Sentinel-2 and -3. *Int. J. Appl. Earth Obs. Geoinformation* **2013**, *23*, 344–351, doi:10.1016/j.jag.2012.10.008.
19. Gitelson, A.A.; Merzlyak, M.N. Quantitative Estimation of Chlorophyll-a Using Reflectance Spectra: Experiments with Autumn Chestnut and Maple Leaves. *J. Photochem. Photobiol. B* **1994**, *22*, 247–252, doi:10.1016/1011-1344(93)06963-4.
20. Horler, D.N.H.; Dockray, M.; Barber, J. The Red Edge of Plant Leaf Reflectance. *Int. J. Remote Sens.* **1983**, *4*, 273–288, doi:10.1080/01431168308948546.
21. Brodersen, C.R.; Vogelmann, T.C. Do Changes in Light Direction Affect Absorption Profiles in Leaves? *Funct. Plant Biol.* **2010**, *37*, 403–412, doi:10.1071/FP09262.
22. Liu, J.; van Iersel, M.W. Photosynthetic Physiology of Blue, Green, and Red Light: Light Intensity Effects and Underlying Mechanisms. *Front. Plant Sci.* **2021**, *12*, 619987, doi:10.3389/fpls.2021.619987.
23. Demmig-Adams, B. Survey of Thermal Energy Dissipation and Pigment Composition in Sun and Shade Leaves. *Plant Cell Physiol.* **1998**, *39*, 474–482, doi:10.1093/oxfordjournals.pcp.a029394.
24. Jiang, C.-D.; Gao, H.-Y.; Zou, Q.; Jiang, G.-M.; Li, L.-H. Leaf Orientation, Photorespiration and Xanthophyll Cycle Protect Young Soybean Leaves against High Irradiance in Field. *Environ. Exp. Bot.* **2006**, *55*, 87–96, doi:10.1016/j.envexpbot.2004.10.003.
25. Takahashi, S.; Badger, M.R. Photoprotection in Plants: A New Light on Photosystem II Damage. *Trends Plant Sci.* **2011**, *16*, 53–60, doi:10.1016/j.tplants.2010.10.001.
26. Filella, I.; Porcar-Castell, A.; Munné-Bosch, S.; Bäck, J.; Garbulsky, M.F.; Peñuelas, J. PRI Assessment of Long-Term Changes in Carotenoids/Chlorophyll Ratio and Short-Term Changes in de-Epoxidation State of the Xanthophyll Cycle. *Int. J. Remote Sens.* **2009**, *30*, 4443–4455, doi:10.1080/01431160802575661.
27. Hernández-Clemente, R.; Hornero, A.; Mottus, M.; Penuelas, J.; González-Dugo, V.; Jiménez, J.C.; Suárez, L.; Alonso, L.; Zarco-Tejada, P.J. Early Diagnosis of Vegetation Health From High-Resolution Hyperspectral and Thermal Imagery: Lessons Learned From Empirical Relationships and Radiative Transfer Modelling. *Curr. For. Rep.* **2019**, *5*, 169–183, doi:10.1007/s40725-019-00096-1.
28. Möttus, M.; Hernández-Clemente, R.; Perheentupa, V.; Markiet, V. In Situ Measurement of Scots Pine Needle PRI. *Plant Methods* **2017**, *13*, 35, doi:10.1186/s13007-017-0184-4.
29. Peguero-Pina, J.J.; Camarero, J.J.; Abadía, A.; Martín, E.; González-Cascón, R.; Morales, F.; Gil-Pelegrín, E. Physiological Performance of Silver-Fir (*Abies Alba* Mill.) Populations under Contrasting Climates near the South-Western Distribution Limit of the Species. *Flora Morphol. Distrib. Funct. Ecol. Plants* **2007**, *202*, 226–236, doi:10.1016/j.flora.2006.06.004.
30. Wong, C.Y.S.; Gamon, J.A. Three Causes of Variation in the Photochemical Reflectance Index (PRI) in Evergreen Conifers. *New Phytol.* **2015**, *206*, 187–195, doi:10.1111/nph.13159.
31. Cirillo, V.; D'Amelia, V.; Esposito, M.; Amitrano, C.; Carillo, P.; Carputo, D.; Maggio, A. Anthocyanins Are Key Regulators of Drought Stress Tolerance in Tobacco. *Biology* **2021**, *10*, 139, doi:10.3390/biology10020139.
32. Landi, M.; Tattini, M.; Gould, K.S. Multiple Functional Roles of Anthocyanins in Plant-Environment Interactions. *Environ. Exp. Bot.* **2015**, *119*, 4–17, doi:10.1016/j.envexpbot.2015.05.012.
33. Steyn, W.J.; Wand, S.J.E.; Holcroft, D.M.; Jacobs, G. Anthocyanins in Vegetative Tissues: A Proposed Unified Function in Photoprotection. *New Phytol.* **2002**, *155*, 349–361.
34. Gould, K.S. Nature's Swiss Army Knife: The Diverse Protective Roles of Anthocyanins in Leaves. *J. Biomed. Biotechnol.* **2004**, *2004*, 314–320, doi:10.1155/S1110724304406147.
35. Kyparissis, A.; Grammatikopoulos, G.; Manetas, Y. Leaf Morphological and Physiological Adjustments to the Spectrally Selective Shade Imposed by Anthocyanins in *Prunus Cerasifera*. *Tree Physiol.* **2007**, *27*, 849–857, doi:10.1093/treephys/27.6.849.

36. Hernández, I.; Alegre, L.; Van Breusegem, F.; Munné-Bosch, S. How Relevant Are Flavonoids as Antioxidants in Plants? *Trends Plant Sci.* **2009**, *14*, 125–132, doi:10.1016/j.tplants.2008.12.003.
37. Stimson, H.C.; Breshears, D.D.; Ustin, S.L.; Kefauver, S.C. Spectral Sensing of Foliar Water Conditions in Two Co-Occurring Conifer Species: *Pinus Edulis* and *Juniperus Monosperma*. *Remote Sens. Environ.* **2005**, *96*, 108–118, doi:10.1016/j.rse.2004.12.007.
38. Dao, P.D.; He, Y.; Proctor, C. Plant Drought Impact Detection Using Ultra-High Spatial Resolution Hyperspectral Images and Machine Learning. *Int. J. Appl. Earth Obs. Geoinformation* **2021**, *102*, 102364, doi:10.1016/j.jag.2021.102364.
39. Andrews, S.F.; Flanagan, L.B.; Sharp, E.J.; Cai, T. Variation in Water Potential, Hydraulic Characteristics and Water Source Use in Montane Douglas-Fir and Lodgepole Pine Trees in Southwestern Alberta and Consequences for Seasonal Changes in Photosynthetic Capacity. *Tree Physiol.* **2012**, *32*, 146–160, doi:10.1093/treephys/tpr136.
40. Irvine, J.; Perks, M.P.; Magnani, F.; Grace, J. The Response of *Pinus Sylvestris* to Drought: Stomatal Control of Transpiration and Hydraulic Conductance. *Tree Physiol.* **1998**, *18*, 393–402, doi:10.1093/treephys/18.6.393.
41. Black, K.; Philk, D.; Mc Grath, J.; Doherty, P.; Bruce, O. Interactive Effects of Irradiance and Water Availability on the Photosynthetic Performance of *Picea Sitchensis* Seedlings: Implications for Seedling Establishment under Different Management Practices. *Ann. For. Sci.* **2005**, *64*, 219–228, doi:10.1051/forest.
42. Matisons, R.; Krišāns, O.; Jansons, Ā.; Kondratovičs, T.; Elferts, D.; Ievinsh, G. Norway Spruce Seedlings from an Eastern Baltic Provenance Show Tolerance to Simulated Drought. *Forests* **2021**, *12*, 82, doi:10.3390/f12010082.
43. Hetherington, A.M.; Woodward, F.I. The Role of Stomata in Sensing and Driving Environmental Change. *Nature* **2003**, *424*, 901–908, doi:10.1038/nature01843.
44. Ensminger, I.; Yao-Yun Chang, C.; Bräutigam, K. Tree Responses to Environmental Cues. In *Advances in Botanical Research*; Elsevier, 2015; Vol. 74, pp. 229–263 ISBN 978-0-12-398548-4.
45. Balekoglu, S.; Caliskan, S.; Dirik, H.; Rosner, S. Response to Drought Stress Differs among *Pinus Pinea* Provenances. *For. Ecol. Manag.* **2023**, *531*, 120779, doi:10.1016/j.foreco.2023.120779.
46. López, R.; Rodríguez-Calcerrada, J.; Gil, L. Physiological and Morphological Response to Water Deficit in Seedlings of Five Provenances of *Pinus Canariensis*: Potential to Detect Variation in Drought-Tolerance. *Trees - Struct. Funct.* **2009**, *23*, 509–519, doi:10.1007/s00468-008-0297-5.
47. Sánchez-Gómez, D.; Velasco-Conde, T.; Cano-Martín, F.J.; Ángeles Guevara, M.; Teresa Cervera, M.; Aranda, I. Inter-Clonal Variation in Functional Traits in Response to Drought for a Genetically Homogeneous Mediterranean Conifer. *Environ. Exp. Bot.* **2011**, *70*, 104–109, doi:10.1016/j.envexpbot.2010.08.007.
48. Taïbi, K.; Del Campo, A.D.; Vilagrosa, A.; Bellés, J.M.; López-Gresa, M.P.; Pla, D.; Calvete, J.J.; López-Nicolás, J.M.; Mulet, J.M. Drought Tolerance in *Pinus Halepensis* Seed Sources As Identified by Distinctive Physiological and Molecular Markers. *Front. Plant Sci.* **2017**, *8*, 1202, doi:10.3389/fpls.2017.01202.
49. Grant, O.M.; Montero Ribeiro, A.F.; Glombik, P.; O'Reilly, C. Impact of Limited Water Availability on Growth and Biomass Production of a Range of Full-Sibling Sitka Spruce (*Picea Sitchensis* (Bong.) Carr.) Families. *For. Int. J. For. Res.* **2018**, *91*, 83–97, doi:10.1093/forestry/cpx034.
50. Čepl, J.; Stejskal, J.; Lhotáková, Z.; Holá, D.; Korecký, J.; Lstibůrek, M.; Tomášková, I.; Kočová, M.; Rothová, O.; Palovská, M.; et al. Heritable Variation in Needle Spectral Reflectance of Scots Pine (*Pinus Sylvestris* L.) Peaks in Red Edge. *Remote Sens. Environ.* **2018**, *219*, 89–98, doi:10.1016/j.rse.2018.10.001.
51. George, J.-P.; Grabner, M.; Campelo, F.; Karanitsch-Ackerl, S.; Mayer, K.; Klumpp, R.T.; Schüler, S. Intra-Specific Variation in Growth and Wood Density Traits under Water-Limited Conditions: Long-Term-, Short-Term-, and Sudden Responses of Four Conifer Tree Species. *Sci. Total Environ.* **2019**, *660*, 631–643, doi:10.1016/j.scitotenv.2018.12.478.
52. Barakat, M.; El-Hendawy, S.; Al-Suhaibani, N.; Elshafei, A.; Al-Doss, A.; Al-Ashkar, I.; Ahmed, E.; Al-Gaadi, K. The Genetic Basis of Spectral Reflectance Indices in Drought-Stressed Wheat. *Acta Physiol. Plant.* **2016**, *38*, 227, doi:10.1007/s11738-016-2249-9.
53. El-Hendawy, S.E.; Alotaibi, M.; Al-Suhaibani, N.; Al-Gaadi, K.; Hassan, W.; Dewir, Y.H.; Emam, M.A.E.-G.; Elsayed, S.; Schmidhalter, U. Comparative Performance of Spectral Reflectance Indices and Multivariate

Modeling for Assessing Agronomic Parameters in Advanced Spring Wheat Lines Under Two Contrasting Irrigation Regimes. *Front. Plant Sci.* **2019**, *10*, 1537, doi:10.3389/fpls.2019.01537.

54. Ensminger, I.; Sveshnikov, D.; Campbell, D.A.; Funk, C.; Jansson, S.; Lloyd, J.; Shibistova, O.; Öquist, G. Intermittent Low Temperatures Constrain Spring Recovery of Photosynthesis in Boreal Scots Pine Forests. *Glob. Change Biol.* **2004**, *10*, 995–1008, doi:10.1111/j.1365-2486.2004.00781.x.
55. Qi, Y.; Dennison, P.E.; Jolly, W.M.; Kropp, R.C.; Brewer, S.C. Spectroscopic Analysis of Seasonal Changes in Live Fuel Moisture Content and Leaf Dry Mass. *Remote Sens. Environ.* **2014**, *150*, 198–206, doi:10.1016/j.rse.2014.05.004.

Disclaimer/Publisher's Note: The statements, opinions and data contained in all publications are solely those of the individual author(s) and contributor(s) and not of MDPI and/or the editor(s). MDPI and/or the editor(s) disclaim responsibility for any injury to people or property resulting from any ideas, methods, instructions or products referred to in the content.